Preprints of the 21st IFAC World Congress (Virtual)
Berlin, Germany, July 12-17, 2020

Minimally Invasive Model Based Stressed Blood Volume as an Index of Fluid Responsiveness

L. F Murphy * **J. G Chase** ** **S. M Davidson** *** **R. Smith** ****
T. Desaive †

* *Department of Mechanical Engineering, University of Canterbury, Christchurch, NZ (e-mail: liam.murphy@ pg.canterbury.ac.nz).*
** *(e-mail: geoff.chase@canterbury.ac.nz)*
*** *Institute of Biomedical Engineering, University of Oxford, United Kingdom (e-mail: shaundavidson.research@gmail.com)*
**** *(e-mail: rachel.smith@ pg.canterbury.ac.nz)*
† *Liege University, Liege, Belgium (e-mail: tdesaive@uliege.be]*

Abstract: Model based total stressed blood volume (SBV_T) has been shown to be a potential index of fluid responsiveness. However, current models rely on the availability of highly invasive and uncommon measurements to derive model parameters. In this work, a simple method for obtaining the necessary model parameters from currently available intensive care unit (ICU) measurements is established. The model is tested on three (3) porcine subjects administered a typical 500ml saline bolus fluid therapy and then subjected to endotoxin induced sepsis to provide a range of hemodynamic states. When compared to stressed blood volume derived from a model utilising direct measurements mean percentage error was 10.3% over a total of 716 beats. This work also examined the hypothesis a stressed blood volume below a clinically specified threshold of 145ml would yield a positive response. Increases of 37.9%, 44.7% and 22.6%, with baseline levels of 180, 120 and 75ml, were seen for pigs 1, 2 and 3, respectively. This research demonstrates the clinical validity of this model based SBV_T measure, bringing it closer to clinical feasibility.

Keywords: Cardiovascular, Stressed Blood Volume, Sepsis, Perfusion, Shock, Fluid Responsiveness

1. INTRODUCTION

Sepsis is a disease causing an inappropriate inflammatory response to an infection resulting in ischemia, hypotension, multiple organ failure, and potentially death. Sepsis and septic shock is the the 10th leading cause of death in the US with an estimated cost of $16.7 billion annually (Merx and Weber (2007)). However, treatment has remained a challenge with significant variability. Thus, there is a need for accurate monitoring enabling effective treatment.

Current treatment of sepsis is guided by the Surviving Sepsis campaign (Dellinger et al., 2013). However, these goal directed therapies have been shown to have no significant impact on patient well-being compared to standard care (Zhang et al., 2017), leading to inconsistent treatment. While exact details on treatments vary, fluid resuscitation is a common component.

The Surviving Sepsis campaign suggests $30 ml/kg$ of fluids during the initial resuscitation phase (Dellinger et al., 2013). However, approximately 50% of patients who receive fluid therapy are non responsive. Furthermore, there is increasing evidence excessive fluids have a deleterious effect (Mackenzie and Noble (2014)). Accurately monitoring and predicting patient-specific response to fluid therapy is therefore critical, but requires insight to patient condition which is currently unavailable.

Total Stressed Blood Volume (SBV_T) has recently been shown to be one such potential index of fluid responsiveness (Pironet et al., 2015). SBV_T is defined as '*the total pressure generating blood volume in the circulation*' (Maas et al. (2012)). SBV_T is the difference between the total volume in the circulation in the minimum volume required to fill blood vessels to the point a force is applied to the vessel wall. It thus influences venous return and is a direct potential measure of tissue perfusion, two metrics of importance in treating sepsis. SBV_T has a negative correlation with fluid responsiveness ((Pironet et al., 2015)).

However, direct measurement of SBV_T requires multiple cardiac arrests and fluid boluses. These procedures make it unethical to measure directly, creating a need for a real-time model based analogue. (Pironet et al. (2015)) first introduced a lumped three chambered cardiovascular system model which outputs a set of parameters, one of which is SBV_T. Figure 1 shows the model schematic.

This model still requires a number of measurements, including: Aortic Pressure, Left Ventricle Volume, Left Ventricle Pressure, Central Venous Pressure, Stroke Volume.

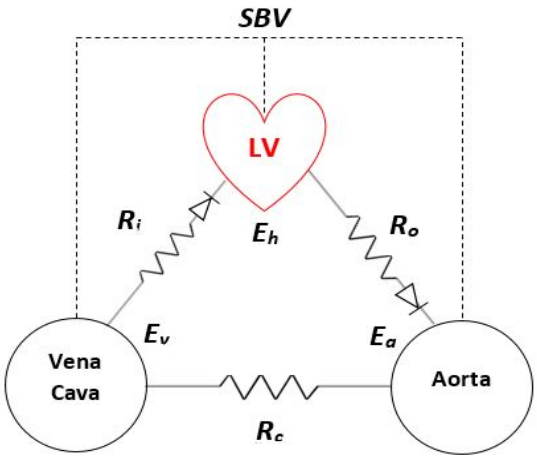

Fig. 1. Schematic of the Three Chambered Cardiovascular System model with relevant parameters.

Left ventricle pressure and volume are not typically available in the ICU and require highly invasive procedures. Direct measurement of aortic pressure is also uncommon. Thus, for the model to be considered clinically applicable SBV_T must be able to be estimated from currently available measurements. This work investigates a method for deriving real time monitoring of SBV_T from measurements currently available in the ICU.

2. METHODS

2.1 Three Chambered Model

The cardiovascular system model used was introduced by ((Pironet et al., 2015)) per Figure 1. The model consists of three (3) elastic chambers: the left ventricle, *lv*, aorta, *ao*, and one vena cava, *vc*, and three flow resistances: input and output cardiac resistance,*Ri* and *Ro*, respectively, and systemic circulation resistance, *Rc*. Pressure-volume relation ships of each chamber are defined:

$$P_x(t) = E_x \times V_{s,x}, \qquad where \quad x = lv,\ ao\ or\ vc \tag{1}$$

Where V_s is the stressed blood volume in the corresponding chamber. Stressed blood volume is defined as the total volume minus the unstressed volume V_u. Flows between chambers cross resistances and are defined by upstream and downstream pressures, P_{up} and P_{down}:

$$Q_y(t) = \frac{P_{up,y} - P_{down,y}}{R_y} \qquad where \quad y = i,\ o\ or\ c \tag{2}$$

The continuity equation gives the rate of change of the unstressed volume in each chamber form the flows.

$$\frac{dV_{s,x}(t)}{dt} = Q_{up,y}(t) - Q_{down,y}(t) \tag{3}$$

Total stressed blood volume in the system is a constant therefore, summing the rate of change of each chamber must equal zero.

$$V_{s,lv}(t) + V_{s,vc}(t) + V_{s,ao}(t) = SBV(t) \tag{4}$$

A detailed derivation may be found in (Pironet et al. (2015), Pironet et al. (2017)). It should be noted that over time SBV will change due to a number of factors including the status of the disease or internal conditions i.e. capillary leak. However, over one cardiac cycle SBV can be considered constant. Evaluating SBV periodically allows patient condition to be monitored over time. Initial values for each parameter ($E_{ao}, E_{vc}, E_{lv}, R_i, R_c, R_c$ *and* $V_{s,3}$) are calculated using equations detailed in Pironet et al. (2017). Not all parameters are sensitive enough to be identified because of their relatively low impact on the error function used for parameter identification. A subset selection algorithm utilising the Hessian matrix is used to evaluate the sub set of parameters to be identified. Parameter identification in this work was completed using MATLAB's (The Mathworks, Natick, MA, USA) *fmincon* function.

2.2 Central Blood Pressure Estimation

Central blood pressure provides vital information about the cardiovascular system, but direct measurement of aortic pressure is highly invasive and uncommon in the ICU. Methods based on transmission line theory have been developed to obtain central blood pressure from peripheral measurements taken (Swamy et al., 2008).

In this work, the arterial tree is modelled as a series of parallel, frictionless tubes each with a characteristic impedance (Z_c). Each tube has a terminal load with a frequency dependent impedance $Z_i(\omega)$. $Z_i(\omega)$ is characterized by a pole-zero structure where $0 \leq A_i \leq B_i$ and defined:

$$Z_i(\omega) = \frac{Z_{ci}(j\omega + B_i)}{j\omega + A_i} \tag{5}$$

Pressure waves are propagated from the aorta, and travel down the tube to the peripheral artery without distortion. At the arterial bed, waves are reflected and travel back towards the aorta with magnitude proportional to the forward wave multiplied by a reflection coefficient:

$$\Gamma_i(\omega) = \frac{Z_i(\omega) - Z_{ci}}{Z_i(\omega) + Z_{ci}} \tag{6}$$

Forward and backward waves are out of phase by time constant (T_i) representing pulse transit time from aorta to femoral artery (Swamy et al., 2008). Using the relationship between forward and back waves an equation for pressure at any point on the arterial tree can be defined:

$$P_i(x, jw) = P_{fi}(0, jw)\left[e^{jwT_{di}\frac{x}{d_i}} + \Gamma_i(j\omega)e^{-jwT_{di}\frac{x}{d_i}}\right] \tag{7}$$

Combining Equations 5, 6 and 7 a transfer function relating the pressure at the aorta to the femoral artery can be developed. Similarly a transfer function relating the flow and pressure at the femoral artery is obtained. Inverse transformation and discretization of the subsequent transfer functions, using a backwards Euler method, provides the discrete time transfer functions defined:

$$\begin{aligned} p_{ai}[n] = \alpha_i p_a[n-1] + \beta_i p_{pi}[n + N_{di}] - \alpha_i p_{pi}[n + N_{di} - 1] \\ + (1 - \beta_i)\, p_{pi}[n - N_{di}] \end{aligned} \tag{8}$$

$$q_{ai}[n] = \frac{1}{Z_{ci}}\alpha_i q_{ai}[n-1] + \beta_i p_{pi}[n+N_{di}] - \alpha_i p_{pi}[n+N_{di}-1] - (1-\beta_i)\, p_{pi}[n-N_{di}] \quad (9)$$

where n is the discrete time step; N_{di} is the number of samples in the time T_d; and $\alpha_i = F_s/(B_i + F_s)$ and $\beta_i = ((B_i + A_i)/2 + F_s)/(B_i + F_s)$. F_s is the sampling frequency and α and β exist in the range of $0 < \alpha < \beta < 1$. Values for α and β are computed using a parametric grid search and prior knowledge of the aortic pressure and flow. Previous methods have used a single selection criteria for the parameter identification with the caveat being the result must be physiologically reasonable. This work utilised the following criteria:

(1) Pressure displays an exponential decay during diastole
(2) Flow is negligible during diastole
(3) Flow regurgitation is less than 50% maximum flow

Pressure and flow transfer functions differ by a sign in the numerator, stating pressure waves add, while flow waves subtract, and a Z_{ci} in the denominator.

2.3 Driver Function Model

Time varying elastance (TVE) curves are commonly implemented as driver functions. They represent the active elastance of the cardiac chamber and are defined:

$$e(t) = \frac{P_{lv}(t)}{V_{lv}(t) - V_u} \quad (10)$$

where V_u is the unstressed volume in the left ventricle and P_{lv} and V_{lv} are the left ventricle pressure and volume, respectively. A method first introduced by (Davidson et al., 2017a) is used approximate the driver function from the estimated central blood pressure end systolic volume V_{es} and stroke volume (SV). Using simple physiological assumptions, the variables in Equation 10 can be determined.

To approximate P_{lv} it is assumed aortic valve resistance is negligible. Thus, for the majority of systole P_{lv} can be equated to aortic pressure (P_{ao}). During diastole P_{lv} can be modelled with an exponential increase during contraction and an exponential decrease during relaxation. P_{lv} is defined:

$$P_{lv} = \begin{cases} P_a(t_1 + \delta < t < t_2 + \delta) & t_1 < t < t_2 \\ 6 + (P_{a(t_2)} - 6)e^{-17.5(t-t_2)} & t_2 < t < t_3 \\ P_{lv}(t_3) + (P_a(t_4) & \\ -P_{lv}(t_3))e^{37.5(t-t_4)} & t_3 < t < t_4 \end{cases} \quad (11)$$

where $\delta = 0.008s$ and is the phase lag between the aortic and left ventricle pressure curves. Timings of various cardiac events used to map central pressure to left ventricle pressure are given by:

$$t_1 = t\left(\frac{dP_a}{dt}_{max}\right)_n \quad (12)$$

$$t_2 = t\left(\frac{dP_a}{dt}_{min}\right)_n \quad (13)$$

$$t_3 = t\left(P_a\right)_{min} \quad (14)$$

$$t_4 = t\left(\frac{dP_a}{dt}_{max}\right)_{n+1} \quad (15)$$

The V_{lv} waveform is approximated using a piecewise sine wave with a 90° phase shift in conjunction with 6 pieces of information derived from the aortic pressure waveform, 3 timings and 3 volumes associated with diastole and systole. Using a baseline measurement for end-systolic volume the unstressed volume V_u can be estimated:

$$V_u = 0.48 \times V_{es} \quad (16)$$

Continuous end-systolic volume can then be approximated using the pressure volume relationship (Davidson et al., 2017b):

$$P_{DN} = (E_c \times HR^3) \times (V_{es} - V_u) \quad (17)$$

Development of Equation 17 is based on the following physiological assumptions:

- Pressure in the ventricle and aorta are approximately equal until valve closure
- Ventricle volume at zero pressure and unstressed volume are approximately equal

Finally V_{lv} is approximated by:

$$V_{lv}(t) = \begin{cases} (V_{ed})_n + ((V_{es})_n - (V_{ed})_n) & \\ \times \sin\left(\frac{\pi(t-t_1)}{2(t_2-t_1)}\right) & t_1 < t < t_2 \\ (V_{es})_n + ((V_{ed})_{n+1} - (V_{ed})_n) & \\ \times \left(\frac{1}{2}\cos\left(\frac{\pi(t-t_2)}{(t_3-t_2)}\right) - \frac{1}{2}\right) & t_2 < t < t_3 \end{cases} \quad (18)$$

Where:

$$t_1 = t(P_{a_{min}})_n \quad (19)$$

$$t_2 = t(P_{DN})_n \quad (20)$$

$$t_3 = t(P_{a_{min}})_{n+1} \quad (21)$$

$$V_{ed} = V_{es} + SV \quad (22)$$

Where Equations 19 - 21 are the timings of various cardiac events used to map central pressure to left ventricle volume.

2.4 Stroke Volume Estimation

Stroke volume (SV) is estimated using a three element windkessel model, which utilizes the femoral pressure wave to approximate aortic flow and SV (Balmer et al., 2019). The measured femoral pressure is the summation of the

reservoir pressure, $P_{res}(t)$, and the pressure drop associated with blood ejecting from the ventricle, $P_{ex}(t)$ defined:

$$P_{mea}(t) = P_{res}(t) + P_{ex}(t) \tag{23}$$

$P_{res}(t)$ can be described in terms of Z, R and C, which represent the characteristic impedance, resistance and capacitance of the electrical circuit equivalent of the arterial tree, receptively. $P_{res}(t)$ is defined:

$$P_{res}(t) =$$

$$e^{-\lambda t}\left(\int_0^t \left[e^{\lambda t}\left(\frac{P_{mea}(\tau)}{ZC} + \frac{P_{cvp}(\tau)}{RC}\right)\right] dt \; + P_{mea}(0)\right]$$

where:

$$\lambda = \frac{1}{ZC} + \frac{1}{RC} \tag{24}$$

ZC and RC are identified from the femoral pressure wave during diastole. Here it is known $P_{ex} = 0$ leading to the following condition:

$$P_{res}(t > td) = P_{mea}(t > td) \tag{25}$$

where t_d is the time ventricular ejection ends and diastole begins. Start and end systole are then identified through feet detection and a weighted second derivative of the peak pressure to end diastole region, respectively.

Start and end systole are found by determining the feet location of the femoral pressure and the maxima of the weighted second derivative from peak pressure to end diastole, respectively. Combining Equations 23, 24 and 25 and integrating results in an estimate for stroke volume:

$$SV_{est} = \frac{1}{Z}\int_0^t P_{ex}(\tau)d\tau \tag{26}$$

2.5 Experimental Data

The experimental protocol was approved by the Ethics Committee for use of animals at the University of Liege, Belgium (Reference Number 14-1726). Six (6) pure Pietrain pigs were anaesthetised and mechanically ventilated. Septic shock was then induced in the subjects via a one off infusion of endotoxin (lipopolysaccharide from *E. Coli*, 0.5 mg/kg infused over 30 min). Pre-endotoxin infusion, a 500 mL saline solution is first administered over 30 min simulating fluid resuscitation therapy. Aortic pressure in the subjects is continually measured via a catheter with a sampling rate of 250 Hz. P_{lv} and V_{lv} are also continually measured at a rate of 250 Hz via an admittance pressure volume catheter inserted into the left ventricle via an apical stab.

3. RESULTS

Figure 2 shows an example of measured left ventricle, aortic and central venous pressure (red) compared to the model output after parameter identification. These results show the ability of the model to accurately identify parameters and describe the cardiovascular system, including SBV_T. Table 2 details the percentage of the area-error-under-the-curve of left ventricle, aortic and central venous pressure with mean errors 14.1%, 8.5% and 13.3%, respectively. Errors were calculated according to:

$$\epsilon_{abs} = \frac{\int_0^1 |sim(t) - meas(t)|}{\int_0^1 meas(t)} \tag{27}$$

Where *sim* is the model output using measurements available in an ICU and *mea* is the model output utilising a fully measured set of model inputs.
Table 1 details the error in SBV_T, and other key model outputs, identified using estimates for central blood pressure and stroke volume, compared to the same model utilizing direct measurements for all model inputs. Errors were calculated on a beat for beat basis using Equation 27. The mean percentage errors for model outputs were 10.4%, 3.3% and 14.0% for P_{lv}, P_{ao} and P_{vc}, respectively, calculated from the area-under-the-curve. Mean SBV_T error was 5.3, 4.8 and 20.9 % for Pigs 1, 2 and 3, respectively.

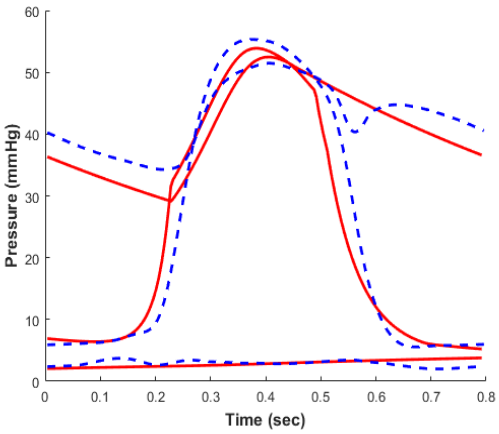

Fig. 2. Example result of the three chamber model's ability to identify parameters describing the cardiovascular system. Red lines are model outputs and blue are measured waveforms

Table 2 details the response of model based SBV_T to fluid therapy and endotoxin induced sepsis. Previously, a positive response to fluid therapy has been defined as an increase in cardiac output $>$ 12%. SBV_T is a relatively new potential index of fluid responsiveness, so $\pm$ 10% was defined as a clinically relevant response. Results matched hypotheses with a mean increase of 35% after fluid therapy and a mean decrease of -14.7% after endotoxin. Pig 3 suffered serious complications after endotoxin administration and died shortly after.

Table 2 also details SBV_T levels prior to fluid therapy. (Pironet et al. (2015)) had shown SBV_T $<$ 145ml was expected to show a positive response to fluid therapy. Pigs 2 and 3 had SBV_T baseline levels of 120 and 75 ml, respectively and both had positive responses to fluids. Pig 1 had a baseline level of 180ml which, while exceeding the 145ml threshold for an expected positive response, presented a positive response, and is still low.

Figure 3 shows the results of identifying SBV_T during fluid resuscitation therapy, endotoxin induced sepsis and

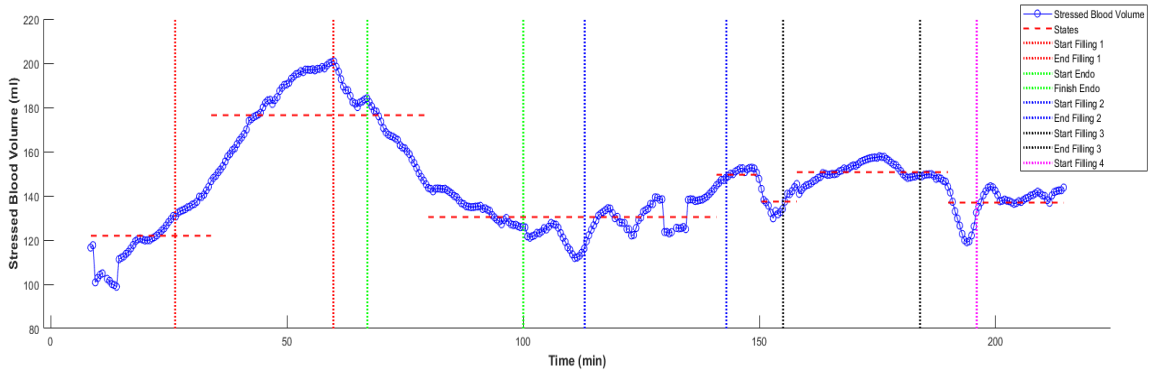

Fig. 3. Model based stressed blood volume of Pig 2 detailing state changes in response to various clinical procedures. Vertical coloured lines represent clinical procedures designed to induce sepsis and simulate treatment.

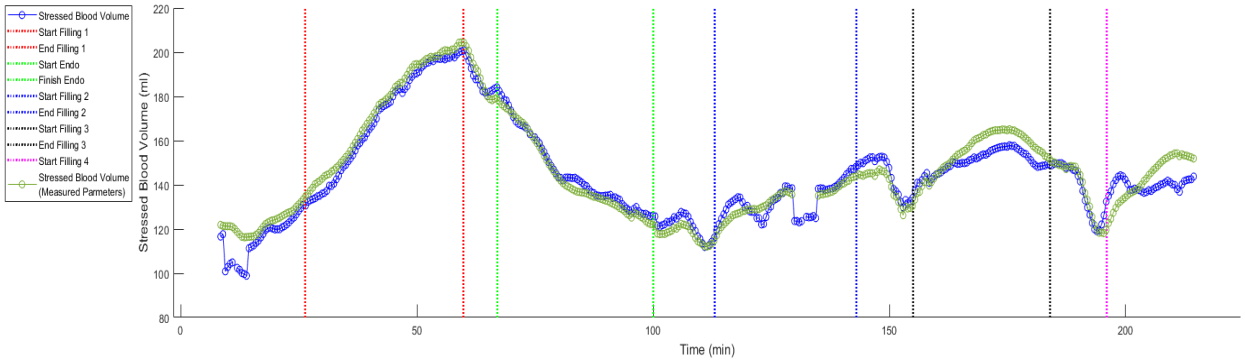

Fig. 4. Comparison of SBV_T estimated using direct measurements and SBV_T estimated from clinically available measurements. Vertical coloured lines represent clinical procedures designed to induce sepsis and simulate treatment.

Table 1. Beat by beat error analysis of three chambered model output compared to directly measured counterparts

Pig	SBV_T (%)	Plv (%)	Pao(%)	Pvc(%)	Sample Size
Pig 1	5.3	14.7	9.2	12.9	176
Pig 2	4.8	14.0	9.3	8.9	413
Pig 3	20.9	13.6	7.0	18.0	127
Mean	10.3	14.1	8.5	13.3	239

Table 2. Results of state analysis on initial fluid therapy and subsequent endotoxin infusion of SBV_T

Pig	SBV Level	Fluid Therapy (%)	Endotoxin(%)
Pig 1	180	+37.9	-16.3
Pig 2	120	+44.7	-13.0
Pig 3	75	+22.6	D
Mean	125	+35.0	-14.7

subsequent fluid therapies. A state average analysis (Zhou et al. (2018)) is used to identify trends in modelled SBV_T, with states denoted by horizontal dashed lines. Vertical lines on Figure 3 represent the start and end time of each of the various procedures. Due to complication during the experiment only three pigs provided data suitable to running a long term trend analysis. These were pigs 1, 2 and 3.

4. DISCUSSION

Fluid therapy aims to increase the cardiac output in a patient and assist with tissue perfusion by increasing the total volume. Thus, an increase in SBV_T is expected to be seen in response to fluid therapy. SBV_T is negatively associated with fluid responsiveness, with a threshold of below 145ml expected to provide a positive fluid response (Pironet et al. (2015)).

Trends in the model output were analysed using a state change analysis, with a $\pm 10\%$ threshold considered clinically significant. It was hypothesised that SBV_T will see an increase in response to fluid therapy and a decrease as the effects of sepsis begin to be felt.

State changes in SBV_T pre and post fluid therapy matched the hypothesis. In all subjects SBV_T increased with initial fluid therapy. Figure 3 shows an initial SBV_T of approximately 120ml, denoted by the first state, indicating the subject is expected to be fluid responsive. After receiving a 500ml saline solution infusion over approximately 30min a state increase of 44.7% is observed. Although an increase is expected, the magnitude may be attributed to the subject yet to experience any diseased state. To this point the subject could be considered healthy with the cardiovascular system operating normally, thus additional fluid may produce a dramatic increase in SBV_T. The two other subjects, Pigs 1 and 3, also saw increases of 37.9% and 22.6%, respectively. While Pig 1 displayed a baseline

SBV_T in excess of the 145ml threshold it could still be considered to be a low value therefore, a positive response is not unexpected.

Pigs 1 and 3 had severe reactions to the endotoxin and the experiment was concluded shortly after administration. However, Pig 2 provided enough data to allow investigation of the response of SBV_T during fluid therapy after sepsis was induced. After endotoxin administration there is a -26.1% drop in SBV_T. Hypolvolemia is characteristic of sepsis and one of the associated reasons for fluid therapy. Thus, this drop in SBV_T is expected. An SBV_T state average of approximately 130ml is seen prior to secondary fluid therapy bolus, which would again indicate a positive response to treatment is expected. Upon being administered the second fluid therapy an increase of 14.9% is observed, indicating fluid responsiveness. A third fluid therapy is administered resulting in a 10% increase in SBV_T which, although diminished, still represents a positive response with a SBV_T of approximately 140ml prior to fluids.

SBV_T modelled in this work utilizes measurements currently available in a clinical setting, and thus requires estimation of some model parameters. Estimation of continuous central blood pressure is derived from continuous femoral artery pressure, through use of the transfer functions in Equation 8. Central blood pressure is required for approximating the left ventricle pressure and volume used to develop cardiac driver functions. Stroke volume is derived from continuous central venous and femoral pressure, as well as baseline measurements of end-diastole volume and aortic flow for calibration.

Estimating model inputs allows wider utilization of the model and eliminates the need for additional, highly invasive measurements. However, estimates inherently present an associated error. Comparison of SBV_T calculated using estimations from clinically available data, and the same methods used with direct measurements of SV and aortic pressure, showed only a modest increase in error, as depicted in Figure 4, and detailed in the first column of Table 1. Absolute percentage error between direct measurements and estimated parameters had mean of of 10.4%, 3.9% and 14.0% for Pigs 1, 2 and 3, respectively. Sample sizes of the experiments were 176, 413 and 127 beats for the respective pigs. This model thus provides an initial proof of concept of clinical validity in these results.

5. CONCLUSION

This work showed a method for identifying stressed blood volume using common ICU measurements, removing the need for additional, highly invasive procedures. When compared to the same model using directly measured values for necessary inputs a mean percentage error in SBV_T of 10.3% over a total of 716 beats was produced. Baseline SBV_T was identified through state analysis to test the hypothesis that SBV_T lower than 145ml was expected to produce a positive response to fluids. Pigs 1, 2 and 3 were seen to have increases in SBV_T of 37.9%, 44.7% and 22.6%, with baseline levels of 180, 120 and 75ml, respectively.

REFERENCES

Balmer, J., Pretty, C.G., Davidson, S., Mehta-Wilson, T., Desaive, T., Smith, R., Shaw, G.M., and Chase, J.G. (2019). Clinically applicable model-based method, for physiologically accurate flow waveform and stroke volume estimation. *Computer Methods and Programs in Biomedicine*, 105125.

Davidson, S., Pretty, C., Pironet, A., Kamoi, S., Balmer, J., Desaive, T., and Chase, J.G. (2017a). Minimally invasive, patient specific, beat-by-beat estimation of left ventricular time varying elastance. *BioMedical Engineering OnLine*, 16(1), 42. doi:10.1186/s12938-017-0338-7. URL `https://doi.org/10.1186/s12938-017-0338-7`.

Davidson, S.M., Pretty, C., Kamoi, S., Balmer, J., Desaive, T., and Chase, J.G. (2017b). Real-time, minimally invasive, beat-to-beat estimation of end-systolic volume using a modified end-systolic pressure-volume relation. *IFAC-PapersOnLine*, 50(1), 5456–5461.

Dellinger, R.P., Levy, M.M., Rhodes, A., Annane, D., Gerlach, H., Opal, S.M., Sevransky, J.E., Sprung, C.L., Douglas, I.S., Jaeschke, R., et al. (2013). Surviving sepsis campaign: international guidelines for management of severe sepsis and septic shock, 2012. *Intensive care medicine*, 39(2), 165–228. doi:10.1007/S00134-012-2769-8.

Maas, J.J., Pinsky, M.R., Aarts, L.P., and Jansen, J.R. (2012). Bedside assessment of total systemic vascular compliance, stressed volume, and cardiac function curves in intensive care unit patients. *Anesthesia & Analgesia*, 115(4), 880–887.

Mackenzie, D.C. and Noble, V.E. (2014). Assessing volume status and fluid responsiveness in the emergency department. *Clinical and experimental emergency medicine*, 1(2), 67.

Merx, M. and Weber, C. (2007). Sepsis and the heart. *Circulation*, 116(7), 793–802. doi: 10.1161/circulationaha.106.678359.

Pironet, A., Dauby, P.C., Chase, J.G., Kamoi, S., Janssen, N., Morimont, P., Lambermont, B., and Desaive, T. (2015). Model-based stressed blood volume is an index of fluid responsiveness. *IFAC-PapersOnLine*, 48(20), 291–296. doi:10.1016/j.ifacol.2015.10.154.

Pironet, A., Docherty, P.D., Dauby, P.C., Chase, J.G., and Desaive, T. (2017). Practical identifiability analysis of a minimal cardiovascular system model. *Computer methods and programs in biomedicine*.

Swamy, G., Mukkamala, R., et al. (2008). Estimation of the aortic pressure waveform and beat-to-beat relative cardiac output changes from multiple peripheral artery pressure waveforms. *IEEE Transactions on Biomedical Engineering*, 55(5), 1521–1529.

Zhang, Z., Hong, Y., Smischney, N.J., Kuo, H.P., Tsirigotis, P., Rello, J., Kuan, W.S., Jung, C., Robba, C., Taccone, F.S., et al. (2017). Early management of sepsis with emphasis on early goal directed therapy: Ame evidence series 002. *Journal of thoracic disease*, 9(2), 392.

Zhou, T., Knopp, J., McKinlay, C.J., Gamble, G.D., Harding, J.E., Chase, J.G., Group, C.S., et al. (2018). Glycaemic state analysis from continuous glucose monitoring measurements in infants. *IFAC-PapersOnLine*, 51(27), 276–281.